

# The Length Scales at Which Classical Elasticity Breaks Down for Various Materials

R. Maranganti, P. Sharma\*

*Department of Mechanical Engineering, University of Houston, Houston, TX 77204*

*Department of Physics, University of Houston, Houston, TX 77204*

(Dated: February 7, 2007)

At what characteristic length scale does classical continuum elasticity cease to accurately describe the small deformation mechanical behavior? The two dominant physical mechanisms that lead to size-dependency of elastic behavior at the nanoscale are surface energy effects and nonlocal interactions. The latter arises due to the discrete structure of matter and the fluctuations in the interatomic forces that are smeared out within the phenomenological elastic modulus at coarser sizes. While the surface energy effect has been reasonably well characterized in the literature, little is known about the length scales at which nonlocal effects manifest for different materials. Using a combination of empirical molecular dynamics and lattice dynamical methods (both empirical and *ab initio*), we provide estimates of the nonlocal elasticity length scales for various classes of materials: semiconductors, metals, amorphous solids and polymers.

PACS numbers: Valid PACS appear here

Classical elasticity is inherently size-independent. Most materials exhibit size-dependent elastic phenomena due to surface energy effects in the length scale range of 1-10 nm [1-3]. This size dependence arises due to the increasing role of surface energies, the effect of which becomes appreciable at the nanoscale due to a large surface-to-volume ratio. However, nonlocality of the stress-strain relationship introduces yet another length scale at which classical elasticity breaks down. A fundamental notion of classical continuum elasticity is that the length scale over which deformation varies is much larger than the discrete length of the matter. This argument would set the breakdown length scale to be in the region of the lattice parameter for most materials. However, discreteness is not the only cause of nonlocality. Long-ranged nature of interatomic forces (say in polar materials) also results in a nonlocal stress-strain relationship. Further, fluctuations in interatomic forces (say for example in amorphous solids) can result in large non-affine displacement fields upon deformation. The characteristic length scale over which the non-affine field is correlated serves as a lower limit beyond which classical continuum elasticity cannot be applied [4]. This characteristic length scale can be significantly higher than the inter-atomic distance. Thus, an assessment of the validity of classical elasticity must figure in accurate interatomic behavior.

The non-local stress-strain behavior can be mimicked in a continuum fashion by including strain-gradient terms in addition to the classical terms to the elastic Lagrangian as shown in Eq. (1)[5-7]

$$L = \frac{1}{2}\rho\dot{u}_i\dot{u}_i - \frac{1}{2}C_{ijkl}e_{ij}e_{kl} - \underbrace{D_{ijklm}u_{i,j}u_{k,lm} - F_{ijklmn}^1u_{i,jk}u_{l,mn} - F_{ijklmn}^2e_{ij}u_{k,lmn}}_{\text{Nonlocal terms}} \quad (1)$$

$\rho$  is the mass density of the solid,  $\mathbf{u}$  is the displacement field; the dot on top of  $u_i$  denotes differentiation with respect to time and the commas denotes differentiation with respect to the spatial variables in the reference configuration.  $\mathbf{e}$  is the symmetric strain tensor. While  $\mathbf{C}$  in Eq. (1) represents the well-known elastic modulus tensor,  $\mathbf{D}$ ,  $\mathbf{F}^1$  and  $\mathbf{F}^2$  are the newly introduced strain-gradient elastic moduli. At larger length scales (assuming small deformations and rotations), the term involving dominates the potential energy and the higher order gradient terms involving the coefficients  $\mathbf{D}$ ,  $\mathbf{F}^1$  and  $\mathbf{F}^2$  provide negligible contributions. However, in the presence of large strain gradients the contributions due to these higher-order terms may prove to be significant and is in fact the *raison d'etre* for this theory. The strain gradients scale inversely with size and thus are expected to cause size-dependency (and hence departure from classical elasticity) at the nanoscale.

From the equations of motion obtained from the Lagrangian of Eq.(1), the dispersion law for  $\omega(\mathbf{k})$  (frequency  $\omega$  vs. wave-vector  $\mathbf{k}$  relation for acoustic waves) can be written as Eq. (2)below:

$$\rho\omega^2u_i^0 = (c_{ijkl}k_jk_l + id_{ijklm}k_jk_lk_m - f_{ijklmn}k_jk_lk_mk_n)u_k^0 \quad (2)$$

Constants  $\mathbf{c}$ ,  $\mathbf{d}$  and  $\mathbf{f}$  are called the dynamic elastic constants and are related to their static counterparts by a set of non-invertible equations.

$$c_{ijkl} = \text{sym}_{(i,k)}\text{sym}_{(j,l)}C_{ijkl} \quad (3)$$

$$d_{ijklm} = \text{asym}_{(i,k)}\text{sym}_{(j,l,m)}D_{ijklm} \quad (4)$$

$$f_{ijklmn} = \text{sym}_{(i,k)}\text{sym}_{(j,l,m,n)}(F_{ijklmn}^2 - F_{ijklmn}^1) \quad (5)$$

The symbols 'sym' and 'asym' respectively denote symmetrization and anti-symmetrization with respect to the indices in the subscripts. For centrosymmetric crystals such as the diamond-like silicon (Si) and germanium (Ge), and f.c.c pure metals copper (Cu) and aluminum (Al), the odd-order tensor  $\mathbf{d}$  vanishes.

\*Electronic address: psharma@uh.edu

Isotropising Eq. (2), the dispersion law can be written as  $\rho\omega^2 = ck^2 - fk^4$ , and the intrinsic length scale parameter associated with the strain-gradient constants can be defined as  $l = \sqrt{f/c}$ . Quantification of the intrinsic length parameter 'l' provides a measure of the length scale at which it is no longer accurate to use classical elasticity. The case of  $l = 0$  corresponds to classical elasticity. At present very little work exists on the evaluation of  $l$  and certainly no clear consensus exists on the variation of  $l$  for various groups of materials and the reasons for why one might be higher than the other.

Eq. (2) of course contains the well known phonon dispersion relations and is typically written as Eq. (6) below.

$$\rho\omega^2 u_i^0 = R_{ik}(k)u_k^0 \quad (6)$$

$R(\mathbf{k})$  is the dynamical matrix derived in a purely elastic continuum framework. In the absence of  $\mathbf{d}$  and  $\mathbf{f}$  (i.e. classical elasticity) from Eq.(2), the relationship between  $\omega$  and  $\mathbf{k}$  would be linear. The terms involving  $\mathbf{d}$  and  $\mathbf{f}$  in Eq.(2) provide a dispersive correction to this linear relationship. Measuring this dispersion can provide an estimate of these non-local dispersive constants. Thus one could, in principle, generate phonon dispersion curves for various materials from either empirical or *ab initio* lattice-dynamics and estimate the values of the independent components of tensors  $\mathbf{d}$  and  $\mathbf{f}$ . However, the identification between the  $3 \times 3$  dynamical matrix obtained via continuum nonlocal elasticity (Eq.6) and the discrete  $3N \times 3N$  dynamical matrix obtained by empirical or *ab initio* lattice dynamics techniques ( $N$  being the number of atoms in the unit cell) is not readily apparent [6]. The  $3N \times 3N$  dynamical matrix obtained by discrete means needs to be block-diagonalized and its  $3 \times 3$  acoustic sub-block can be identified with the  $3 \times 3$  continuum dynamical matrix of Eq.(6); the components of the tensors  $\mathbf{c}$ ,  $\mathbf{d}$  and  $\mathbf{f}$  can be subsequently isolated and the non-local length scales can be extracted. While this can be achieved analytically for empirical for empirical lattice dynamical models [6], the analogous procedure for *ab initio* lattice dynamics has to proceed numerically. The details involved will be discussed in a subsequent publication [8].

Fig.1 shows how the phonon dispersion curves predicted by classical elasticity and non-local elasticity compare with the phonon dispersion curves generated by *ab initio* techniques for copper.

Lattice-dynamics based procedures cannot be employed conveniently to extract the non-local length scale parameters of materials having a non-homogeneous microstructure such as amorphous solids and polymers. In a classical paper by Parrinello and Rahman [10], it was shown that the fluctuations in elastic strain in a  $(\sigma, H, N)$  ensemble (constant stress  $\sigma$ , constant enthalpy  $H$  and constant number of particles  $N$ ) are a direct measure of the elastic compliances (the inverse of which are the classical elastic constants) in a general anisotropic medium. More recently, Meyers et al. [11] (based on Landau and Lifshitz [12] and Pratt [13]) have proposed a method-

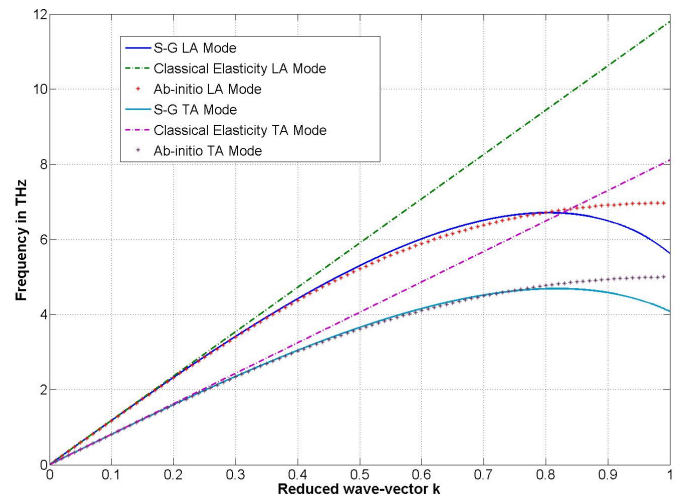


FIG. 1: Shows the comparison of phonon dispersion curves of copper (Cu) predicted by strain-gradient elasticity (S-G modes) and classical elasticity to those obtained by *ab-initio* calculations for the transverse acoustic (TA) and longitudinal acoustic (LA) modes along the [100] symmetry direction.

ology to determine the classical elastic constants of homogeneous solids from the atomic displacement correlation function in an  $NVT$  (constant number of particles  $N$ , constant volume  $V$  and constant temperature  $T$ ) molecular dynamics (MD) ensemble using the long-wavelength approximation. We have extended this technique to be applicable in regime of relatively high-energy wave-vectors so that the dispersive elastic constants can be subsequently extracted from the atomic displacement correlation functions [details to be published in a subsequent publication, Ref. 8]. This method proves advantageous over methods involving strain-strain fluctuations (or stress-stress fluctuations) in that it involves atomic displacements which are easily determined during the course of a simulation as opposed to local strain and stress measures. We have shown [8] that if an  $NVT$  MD simulation is carried out in a cubic simulation box with an edge of length  $L$ , then the thermal average of the displacement correlations can be related to the dynamic elastic constants as:

$$\begin{aligned} & \langle \tilde{u}_i(\mathbf{k}) \tilde{u}_k(-\mathbf{k}) \rangle \\ &= \frac{k_B T}{L^3} (c_{ijkl} k_j k_l + i d_{ijklm} k_j k_l k_m - f_{ijklmnp} k_j k_l k_m k_n)^{-1} \end{aligned} \quad (7)$$

$k_B$  is the Boltzmann constant. To obtain the requisite dynamic elastic constants from Eq. (7), an  $NVT$  MD simulation is carried out at low temperatures for atoms enclosed in a cubic simulation box. The displacements of all the atoms are obtained at each time-step. These displacements in real space can be discrete Fourier-transformed and the correlations given by the left hand-side of Eq. (7) can be calculated for wave-vectors along high-symmetry directions. The thermal average of the displacement correlations can be obtained for different

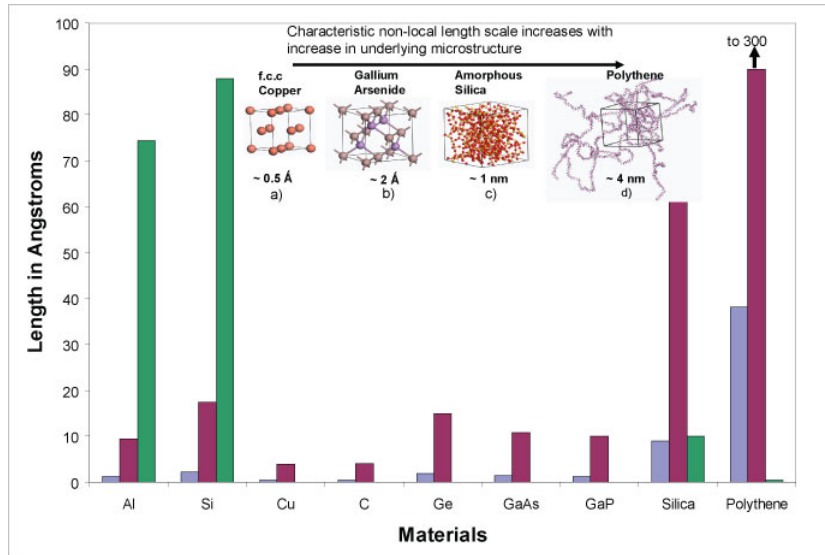


FIG. 2: In the above map pale blue bars represent the larger of the two isotropised non-local length scale parameters for different materials investigated in this work. The magenta bars represent the dimension (breadth) of a beam with a square cross-section (length=10 times the breadth) for which the size-dependent bending rigidity becomes 110% of the Young's modulus for the bulk state as predicted by a model due to Gao et al. [9]. The green bars represent the dimension (breadth) of a beam with a square cross-section for which the size-dependent bending rigidity becomes 10% higher (or 10% lower depending upon the sign of the surface elastic moduli) as predicted by a model incorporating size-dependent surface elastic effects due to Miller and Shenoy [3]. Also shown in the above figure is how the non-local length scale of materials increases with increase in microstructure.

$\mathbf{k}$ -vectors and can be fitted to the right-hand side of Eq. (7) to obtain the dynamic elastic constants  $\mathbf{c}$ ,  $\mathbf{d}$  and  $\mathbf{f}$  from which the non-local length scales can be extracted.

In this work, we have used the three methods described above namely empirical lattice dynamics, *ab initio* lattice dynamics [14] and empirical *NVT* MD [15] to determine the dispersive elastic constants and the associated non-local length scale parameters. For the f.c.c metals Cu and Al we have employed both *ab initio* lattice dynamics and our fluctuations based empirical MD simulation method. For Si we have employed all the three methods i.e. *ab initio* and empirical lattice dynamics and empirical MD. For C (diamond) and GaAs we have used *ab initio* and empirical lattice dynamics to estimate the dispersive constants while for Ge and GaP we have used only empirical lattice dynamics. Lastly, for the non-crystalline systems investigated viz. amorphous silica and polythene only the fluctuations based MD method developed by us is applicable. *Ab initio* phonon dispersions of Cu and diamond (C) were calculated within density-functional perturbation theory in the generalized gradient approximation (GGA). An ultrasoft pseudopotential generated by Favot and Dal Corso [16] using an approach outlined by Kresse and Hafner [17] was employed. *Ab initio* phonon dispersions of Al and Si were calculated in the GGA using a norm-conserving pseudopotential generated by Favot and Dal Corso [16], following the Rappe, Rabe, Kaxiras and Joannopoulos scheme while those of GaAs were calculated in the Local Density Approximation (LDA) using a norm-conserving pseudopotential generated by Giannozzi et al.[18] following a scheme proposed by von

Barth and Car. For the empirical lattice dynamics, Shell Model parameters for Si, Ge and C provided by Price et al.[19] were used. Parameters for the lattice dynamical models of GaAs and GaP have been taken from Kunc et al. [19-21]. While an embedded atom potential [22] was adopted to carry out MD simulations of the metals Cu, Al and Ni, the Tersoff potential [23] was for the semiconductor Si and the Vashishta potential [24] was used to simulate SiO<sub>2</sub>. Empirical MD simulations of multi-component semiconductors like GaAs, AlAs etc. were avoided since reliable inter-atomic potentials are unavailable. All the simulations were carried out at a temperature of 50 K. While the convergence of the elastic constants using this method was found to be slower compared to some other works available in the literature (Ray et al. [25-26]) (typical runs consisted of  $1 \times 10^6$  time-steps each time-step being 1 femto-second) this method was nevertheless employed since it is quite simple to extend Meyers et al.'s [11] technique to include the effects of strain-gradients. Including the effects of strain-gradients is not straightforward in other fluctuation-based techniques to calculate elastic constants: for example the Parrinello and Rahman [10] technique uses a  $(\sigma, H, N)$  ensemble wherein a constant external stress is applied and the fluctuations in the strain (which is the conjugate variable to stress) are in turn related to the classical elastic constants. Trying a similar approach to determine the strain-gradient elastic constants would mean application of an external "couple-stress" (which is the conjugate variable to strain-gradient): how one can achieve this in a computational ensemble is currently unclear. Our main results are en-

compassed in Fig.2 which shows our results for the non-local length scales for various classes of materials.

In light of the results obtained for the dynamic strain gradient constants and associated length scales for the materials investigated, there seems to be a strong indication that classical elasticity is valid for most materials down to a lattice parameter and only breaks down for materials possessing a non-homogeneous microstructure like amorphous silica and polymers. Covalent semiconductors like Si however possess higher non-local length scales compared to metals which may be attributed to the short-ranged nature of inter-atomic forces in metals. The high non-locality in amorphous solids possessing an underlying inhomogeneous microstructure possibly stems from a group of strongly bonded atoms behaving as a unit. Under such circumstances, parts of the material system may undergo considerable non-affine deformation and high moment stresses may result. Since crystalline materials are highly ordered, they very possibly undergo negligible non-affine deformations as a consequence of which the nonlocal elastic effects are unimportant for such systems. Liquid crystal elastomers have also been investigated under the context of Frank elasticity and experimental evidence suggests that their length scales may lie in the 10 nm regime [27]. However, experiments on size-effects on polystyrene by Stafford et al. [28] — through two different methods: thin film wrinkling and nano-indentation—did not reveal any size effects down to 150 nm. A recent work by Nikolov et al. [29] estimated (based on a simple but elegant micromechanical model) that rubbers should have nonlocal length scale in the neighborhood of 4.5 nm. Finally, as far as crystalline systems are concerned, surface elastic effects are the dominant contributors to breakdown of classical continuum elasticity while nonlocal effects are generally negligible.

### Acknowledgments

Financial support from ONR Young Investigator award-N000140510662 is gratefully acknowledged. One of the authors (R. M) would like to thank Xinyuan Zhang for bringing fluctuation-based techniques (to calculate material properties) to his attention. Computational facilities provided by the Texas Learning and Computation Center (TLC<sup>2</sup>) at the University of Houston are highly appreciated.

### References:

1. R.C. Cammarata, Prog. Surf. Sci. 46, 1 (1994)
2. M.E. Gurtin, and A.I. Murdoch, Arch. Ration. Mech. Anal. 57, 291 (1975)
3. R.E. Miller, and V.B. Shenoy, Nanotechnology 11, 139 (2000)
4. F. Leonforte, R. Boissiere, A. Tanguy, J.P. Wittmer, and J.-L. Barrat, Phys. Rev. B. 72, 224206 (2005)
5. R.D. Mindlin, Arch. Rat. Mech. Anal. 16, 51 (1964).
6. D.P.DiVincenzo, Phys. Rev. B. 34, 5450 (1986)
7. X. Zhang, and P. Sharma, Phys. Rev. B. 72, 195345 (2005)
8. R.Maranganti and P. Sharma, Unpublished (2007)
9. X.-L. Gao, J. Micromech. Microeng. 16, 2355 (2006)
10. M. Parrinello, and A. J. Rahman, J. Chem. Phys. 76, 2662 (1982)
11. M.T. Meyers, J.M. Rickman, T.J. Delph, J. Appl. Phys. 98, 066106 (2005)
12. L.D. Landau, and E.M. Lifshitz, Statistical Physics (Course of Theoretical Physics, Volume 5) Part 1. Butterworth-Heinemann (1984)
13. L.R. Pratt, J. Chem. Phys. 87, 1245 (1987)
14. All the *ab initio* phonon calculations were done using the Quantum ESPRESSO package
15. All the MD simulations apart from those with polythene were carried out using GULP. Please refer J.D. Gale, J. Chem. Soc. Faraday T. 93, 629(1997). MD simulations on polythene were carried out using Materials Studio developed by Accelrys Inc.
16. F. Favot, A.Dal Corso, Phys. Rev. B. 60, 427 (1999)
17. G.Kresse, and J. Hafner, J. Phys- Condens. Mat. 6, 8245 (1994)
18. P. Giannozzi, S. de Gironcoli, P. Pavone, and S. Baroni, Phys. Rev. B. 43, 7231 (1991)
19. D.L. Price, J.M. Rowe, and R.M.Nicklrow, Phys. Rev. B. 3, 1268 (1971)
20. Kunc, K., Balkanski, M., and Nusimovici, M. Phys. Stat. Solidi B 71, 341 (1975)
21. Kunc, K., Balkanski, M., and Nusimovici, M. Phys. Stat. Solidi B 72, 229 (1975)
22. F.Cleri, and V. Rosato, Phys. Rev. B. 48, 22 (1993)
23. J.Tersoff, Phys. Rev. Lett. 61, 2879 (1988)
24. P. Vashishta, R.K. Kalia, J.P. Rino, Phys. Rev. B. 41, 12197(1990)
25. J.R. Ray, M.C. Moody, and A. Rahman, Phys. Rev. B. 32, 733(1985)
26. J.R. Ray, M.C. Moody, and A. Rahman, Phys. Rev. B. 33, 895 (1986)
27. M.Warner, Phys. Rev. B. 67, 011701 (2003)
28. C.M. Stafford, S.Guo, C. Harrison, and M.Y.M. Chiang, Rev. Sci. Inst. 76, 062207(2005)
29. S. Nikolov, C.-S.Han, D. Raabe, Int. J. Solids Struct. Doi:10.1016/j.ijsolstr.2006.06.039 (2006)